Specific-heat analysis of rare-earth transition-metal borocarbides: An estimation of the electron-phonon coupling strength

H. Michor, T. Holubar, C. Dusek, and G. Hilscher
Institut für Experimentalphysik, Technische Universität Wien, Wiedner Hauptstrasse 8-10, A-1040 Wien, Austria
(Received 18 May 1995; revised manuscript received 31 July 1995)

We analyzed the superconducting and normal-state heat capacity of superconducting YNi_2B_2C, $LuNi_2B_2C$, $LaPt_{1.5}Au_{0.5}B_2C$ and the nonsuperconducting reference compounds $LaNi_2B_2C$, YCo_2B_2. The deviations of the thermodynamic ratios as $\Delta C/\gamma T_c$, $\gamma T_c^2/H_c^2(0)$, $H_c'(T_c)/T_cH_c(0)$, and $\Delta(0)/k_BT_c$ from their BCS values give an estimate for the strong-coupling parameter $T_c/\omega_{\ln}$ which is in the range of 0.06–0.1 and indicates that the phonon mediated superconductivity can be classified in the moderately strong-coupling limit. From the normal-state specific heat between 2 and 300 K we constructed model phonon spectra to determine the moments of the phonon density of states $F(\omega)$ and calculated the electron-phonon enhancement factor λ with the Allen and Dynes formula which yields λ values in the range of 0.95–1.15 for the three superconducting compounds. The comparison of these λ values with the electron mass enhancement derived from the ratio of the Sommerfeld parameter γ and the calculated density of states at the Fermi level, $N(E_F)$, shows that band structure calculations overestimate $N(E_F)$. Furthermore we determined the upper critical field $H_{c2}(T)$ from specific-heat measurements up to 11 T and the normalized Ginzburg-Landau parameter $k(T)$ which both show BCS-type behavior for $LaPt_{1.5}Au_{0.5}B_2C$, but a significant upward curvature for YNi_2B_2C and especially for $LuNi_2B_2C$.

I. INTRODUCTION

The discovery of superconductivity and its coexistence with magnetism in quaternary transition-metal borocarbides with the formula RNi_2B_2C (R=Y, Ho, Er, Tm, Lu)[1–3] stimulated the research activities of various groups in this field (for a short review see Ref. 4). These compounds crystallize[3] in a filled version of the $ThCr_2Si_2$ structure stabilized by the incorporation of carbon where Ni_2B_2 layers built from NiB_4 tetrahedra are separated by R-C rocksalt layers. Most of the experimental and theoretical results tend to support a conventional BCS description of the superconducting properties. Although a qualitative agreement between band-structure calculations[5–8] and spectroscopic experiments[9–11] is achieved with respect to the density of states (DOS), the spectroscopic experiments indicate that d-d electron correlations play a role and reduce the DOS peak at the Fermi energy predicted by band-structure calculations.

In this paper we present low- and high-temperature specific-heat measurements of superconducting $LuNi_2B_2C$, YNi_2B_2C, $LaPt_{1.5}Au_{0.5}B_2C$, and the nonsuperconducting compounds $LaNi_2B_2C$, YCo_2B_2. The latter compound with the well-known $ThCr_2Si_2$ structure is included to study the influence of carbon upon the phonon contribution to the heat capacity with respect to the borocarbides. $LaPt_{1.5}Au_{0.5}B_2C$ is used to examine the different influence of the $3d$ and $5d$ contribution upon superconductivity. The analysis of the low-temperature specific heat in the superconducting state yields via the BCS ratios, information about the coupling strength λ which can be compared with the electron mass enhancement derived from the ratio of the calculated DOS at E_f and that from the electronic contribution to the heat capacity in the normal state. The heat capacity data up to room temperature provide sufficient information to construct a phonon model density of states from which λ can be calculated with the Allen and Dynes formula.

II. EXPERIMENTAL

Polycrystalline samples of RNi_2B_2C were prepared by high-frequency induction melting and annealing at 1050 °C for 24–36 h (see also Ref. 12). To improve the sample quality we varied the annealing procedure and succeeded to reduce the amount of a secondary phase of $LuNi_2B_2C$ to below 1% by an extended annealing time of three weeks. According to x-ray diffraction and micrographs the improvement of phase purity of the other compounds investigated was limited by secondary phases of about 3–5%. As $LaPt_2B_2C$ could not be obtained as a single-phase material we used $LaPt_{1.5}Au_{0.5}B_2C$ with the proper annealing conditions given by Cava *et al.*[13]

Ac and dc susceptibility measurements were performed in a calibrated ac susceptometer (80 Hz and field amplitudes up to 1 mT) and in a 6 T superconducting quantum interference device magnetometer, respectively. Specific-heat measurements up to 11 T were carried out on 2–3 g samples in three automated calorimeters using a quasiadiabatic step heating technique. In the low-temperature calorimeters (1.5–100 K) the temperature is measured either with a Germanium resistor or with a Carbon glass resistor for zero field and field measurements, respectively, which are situated in the bore of the sapphire sample holder. The field calibration of the latter has been performed *in situ* against a $SrTiO_3$ sensor. For the upper temperature range (80–300 K) we use a thin AuAg disc as sample holder which is surrounded by two active radiation shields in cascade. In addition, the temperatures of the heater and platinum thermometer wires are controlled for minimal residual losses in order to thermally isolate the sample and to obtain proper quasiadiabatic conditions.

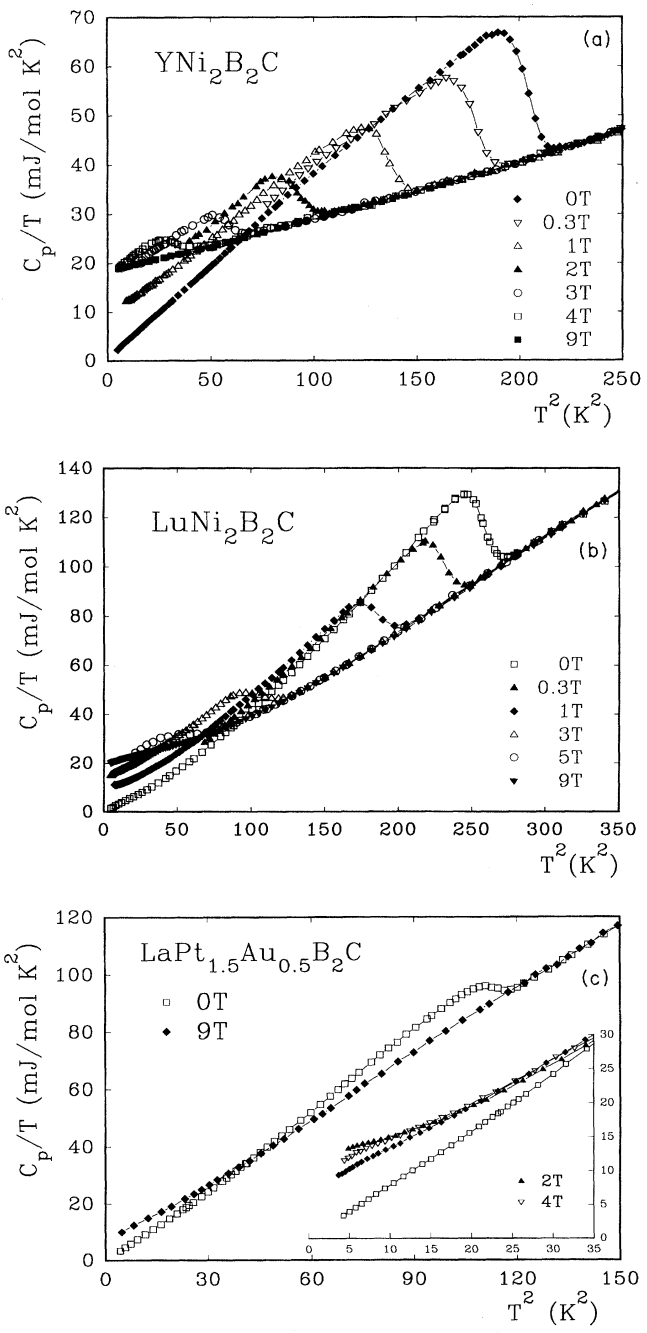

FIG. 1. C_P/T versus T^2 plot for YNi_2B_2C (a), $LuNi_2B_2C$ (b), and $LaPt_{1.5}Au_{0.5}B_2C$ (c) for various external fields as labeled; the inset of Fig. 3(c) shows the significant field dependence of the normal-state heat capacity above 2 T.

III. RESULTS

A. Results of the specific-heat measurements

A comparison of the low-temperature specific heat of YNi_2B_2C, $LuNi_2B_2C$, together with $LaPt_{1.5}Au_{0.5}B_2C$ is shown in a C_P/T versus T^2 representation in Figs. 1(a)–1(c). External fields are applied to suppress superconductivity to determine the normal-state heat capacity $C_P = C_e + C_{ph} = \gamma T + \beta T^3$ where γ is the Sommerfeld parameter and β is related to the low-temperature value of the Debye temperature by $\Theta_D^{LT} = (1944 \times N/\beta)^{1/3}$ (N is the number of atoms per formula unit). From these data in Figs. 1(a)–1(c) all experimental quantities can be deduced which enter into the universal relations predicted by the BCS weak-coupling theory: $H_c(0)/T_c H_c'(T_c) = 0.57$, $\gamma T_c^2/H_c^2(0) = 0.168$, and $(\Delta C)_{T_c}/\gamma T_c = 1.43$, where $(\Delta C)_{T_c} = (C_s - C_n)_{T_c}$ is the specific-heat jump at T_c, $H_c(T)$, and $H_c'(T_c)$ is the thermodynamic critical field and its derivative at T_c. Strong electron-phonon coupling modifies these relations; the magnitude of these corrections was expressed in terms of the strong-coupling parameter $T_c/\bar{\omega}_1$ by Rainer and Bergmann[14] and finally extended to approximate formulas for a large number of superconductors by Marsiglio and Carbotte.[15,16] Thus we present in the following the analysis of the $C_P(T,H)$ data with respect to these quantities to examine the deviations from the aforementioned BCS values which provide a sensitive measure for the coupling strength.

It is obvious from Figs. 1(a)–1(c) that extrapolations from the normal state above T_c gives too small values for γ since the C_P/T vs T^2 plots exhibit a significant deviation from linear behavior below T_c. If, furthermore, the low-temperature heat capacity is dominated by lattice contributions containing some low-energy Einstein modes, the usually employed linearization of these plots may be precarious: The comparison of the normal-state heat-capacity ratios C_e/C_{ph} at 10 K yielding values of about 3, 1, and 0.1 for YNi_2B_2C, $LuNi_2B_2C$, and $LaPt_{1.5}Au_{0.5}B_2C$, respectively, indicates that the uncertainty of the γ value is largest for the latter compound. Additionally, its normal-state heat capacity exhibits a significant field dependence [see inset of Fig. 1(c)] which is not observed for both the Y and Lu compound after suppression of superconductivity in the normal state up to 11 T. In a previous paper[4] we derived for $LaPt_{1.5}Au_{0.5}B_2C$ a γ value of 5.2(6) mJ/mol K^2 from a fit of the low-temperature data with $C_P(T) = \gamma T + C_{Debye}(T)$. The numerical analysis of the specific heat with a more realistic model for the phonon spectrum (see Sec. III B) incorporating not only the Debye spectrum but also low-energy Einstein modes gives $\gamma = 6.4(8)$ mJ/mol K^2. In the case of $LuNi_2B_2C$ the same analysis yields $\gamma = 19.5(3)$ mJ/mol K^2 instead of 18.5(5) mJ/mol K^2 (Ref. 4), while for YNi_2B_2C the Sommerfeld constant [$\gamma = 18.2(2)$ mJ/mol K^2] remains unaffected by this procedure because of the large C_e/C_{ph} ratio of about 3 at low temperatures. These results are collected in Table I where also available data from the literature[17–20] together with band-structure results[5–8] are compiled for a comparison.

The electron mass enhancement (λ) due to electron-phonon interaction and/or electron-electron correlations can be estimated from the ratio of the experimental γ values and the calculated density of states (DOS) at E_f yielding $\gamma/\gamma_{band} = (1+\lambda)$. These values summarized in Table I indicate weak-coupling for $LaPt_{1.5}Au_{0.5}B_2C$ but moderately strong-coupling superconductivity for $LuNi_2B_2C$ and YNi_2B_2C, if all mass enhancement is attributed to electron-phonon interactions. Note that $\lambda \simeq 0.1$ for $LaPt_{1.5}Au_{0.5}B_2C$ is incompatible with a T_c of 10 K which will be discussed in Sec. VI B. Photoemission[9,10] and x-ray-absorption spectroscopy[11] studies have shown that electron correlations

TABLE I. Comparison of the low-temperature specific-heat results for Θ_D^{LT} and γ_{exp} with other available experimental and theoretical results ($\gamma_{band\ structure}$) yielding the given estimate for the mass enhancement λ.

	Θ_D^{LT} (K)	γ_{exp} (mJ/mol K^2)	$\gamma_{band\ structure}$ (mJ/mol K^2)	λ
YNi_2B_2C	490(5)	18.2(2)	9.5[a]	**0.9**
	489(5)[b]	18.7(5)[b]		
	415[c]	8.9[c]		
$LuNi_2B_2C$	360(3)	19.5(3)	11.3[d]	**0.75**
	345(10)[e]	19(2)[e]	11.2(1)[f]	
	350(10)[g]	11(2)[g]		
$LaNi_2B_2C$	495(8)	8.4(3)	6[h]	**0.4**
$LaPt_{1.5}Au_{0.5}B_2C$	250(3)	6.4(8)	5.9[f]	**0.1**
$LaPt_{1.7}Au_{0.3}B_2C$	220(10)[e]	7.5(1.5)[e]	5.9(1)[f]	
YCo_2B_2	570(10)	6.7(1)		

[a]Reference 7.
[b]Reference 17.
[c]Reference 20.
[d]Reference 6.
[e]Reference 18.
[f]Mattheis cited in Ref. 18.
[g]Reference 19.
[h]Reference 33.
[i]Reference 8.

have to be taken into account which reduce the calculated DOS at E_f by a factor of about 0.5.[9] Accordingly, taking this reduction of the DOS at E_f into account, the corrected λ values would place all three compounds into the very strong-coupling regime.

The specific-heat jump $(\Delta C)_{T_c}$ is determined from the zero-field data by assuming an idealized sharp, entropy conserving superconducting transition (see Fig. 2) yielding $\bar{T}_c$ given in Table II. In case of YNi_2B_2C $(\Delta C)_{T_c}$= 460 mJ/mol K is by about 7% larger than our previous value[12] but this is still 6% smaller than that of a single-crystal measurement by Movshovich *et al.*[17]

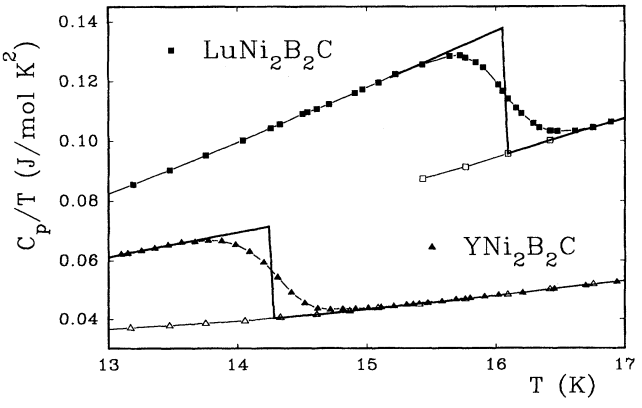

FIG. 2. Specific-heat jump at T_c; the solid line shows the idealized jump under the constraint of entropy conservation. The filled symbols correspond to the zero field and the hollowed symbols to the 9 T measurements.

1. Thermodynamic- and upper critical field and an estimate for the gap-to-critical temperature ratio

The temperature dependence of the upper critical field derived from specific-heat measurements is displayed in Fig. 3 where in the inset the field dependence of the specific-heat jump of $LuNi_2B_2C$ is shown in the low-field regime. Both compounds YNi_2B_2C and $LuNi_2B_2C$ exhibit a significant positive deviation of $\mu_0 H_{c2}(T)$ from the initially linear dependence below 2 T being consistent with magnetic and resistivity measurements. This feature has been already noted for YNi_2B_2C.[4,12,21] As a consequence of this positive deviation, the Werthamer formula $H_{c2}(0) \simeq -0.7 T_c (dH_{c2}/dT)_{T_c}$ underestimates the upper critical field $H_{c2}(0)$ of YNi_2B_2C and $LuNi_2B_2C$ which will be discussed in Sec. IV C. From the low-temperature extrapolation of $H_{c2}(T)$ and the thermodynamic critical field given below we obtain the Ginzburg-Landau parameter $\kappa_1(0) = H_{c2}(0)/[\sqrt{2} H_c(0)] = 16$ for YNi_2B_2C which is significantly higher than our previous value[12] $[\kappa_1(0) = 10.5]$ using the Werthamer formula but is in reasonable agreement with that deduced from magnetic measurements on single crystals by Xu *et al.*[22] $[\kappa_1(0) = 13-15]$ and from the combination of magnetic and μSR data by Cywinski *et al.*[21] $[\kappa_1(0) = 13]$. For $LuNi_2B_2C$ and $LaPt_{1.5}Au_{0.5}B_2C$ we obtain $\kappa_1(0) = 21$ and 7, respectively.

The temperature dependence of the thermodynamic critical field $H_c(T)$ is obtained by integrating the entropy difference between the normal and superconducting state:

$$\frac{\mu_0 H_c^2(T)}{2} = \int_{T_c}^{T} \int_{T_c}^{T'} \frac{(C_s - C_n)}{T''} dT'' dT' . \qquad (1)$$

The application of the above relation to the data in Figs. 1(a)–1(c) (close to T_c we used the idealized data shown in Fig. 2) gives $H_c(T)$, displayed in Fig. 4 from which $H_c'(T_c)$ the slope of H_c at T_c is derived. Note, that for all three compounds the 9 T measurement is used for the normal-state heat capacity. The uncertainty of $H_c(T)$ and its derivative is again largest for the La compound because of the field dependence of the normal-state heat capacity and the more restricted temperature range for the evaluation. Thus, we present in Fig. 5 the deviation function $D(t)$ from the purely quadratic temperature dependence of $H_c(T)$: $D(T/T_c) = D(t) = [H_c(t)/H_c(0)] - [1 - (t)^2]$ for the Y and Lu compound only. As can be seen from the comparison with a BCS superconductor, $LuNi_2B_2C$ exhibits a positive deviation of about 0.7% which is indicative for moderately strong coupling while the deviation for YNi_2B_2C with a small positive and negative deviation can be regarded as typical for medium to moderately strong coupling. A similar shape of $D(t)$ is observed for $LaPt_{1.5}Au_{0.5}B_2C$ with a less pronounced deviation from the parabolic law which, however, is not shown because due to the large phonon contributions to the total heat capacity the evaluation of deviations of $H_c(T)$ of about 1% might overstrain our data. (The lattice heat capacity is at 10 K about ten times larger than the electronic one.)

The shape of the deviation function $D(t)$ can be used to obtain a quantitative estimate of the coupling strength via the gap-to-critical temperature ratio $\Delta(0)/k_B T_c \equiv \alpha$ in terms of the phenomenological α model by Padamsee *et al.*[23] From the comparison of the experimental data in Fig. 5 with the

TABLE II. Calorimetrically determined parameters characterizing the thermodynamic properties of the superconducting borocarbides. The results of Movshovich *et al.* (Ref. 17) on YNi_2B_2C and that of Carter *et al.* (Ref. 18) on $LuNi_2B_2C$ and $LaPt_{1.7}Au_{0.3}B_2C$ are included for comparison.

	YNi_2B_2C	$LuNi_2B_2C$	$LaPt_{1.5}Au_{0.5}B_2C$
$\bar{T}_c$; $T_{c\,\mathrm{onset}}$ (K)	14.25; 14.6	16.1; 16.6	10.65; 10.8
	14.9; 15.2[a]	16.5(1)[b]	10.2(1)[b]
ΔC(mJ/mol K)	460(5)	693(5)	120(15)
	493[a]	561(17)[b]	133(20)[b]
$\Delta C/\gamma T_c$	1.77(4)	2.21(5)	1.8(2)
(BCS: 1.43)	1.77[a]	1.8(2)[b]	1.7(2)[b]
$\mu_0 H_c(0)$(T)	0.229(2)	0.306(3)	0.10(1)
	0.248[a]		
$\mu_0 H_c'(T_c)$(mT/K)	−30.6(5)	−37.5(5)	−18(1)
	−32.4[a]		
$H_c(0)/H_c'(T_c)T_c$	0.53(2)	0.51(1)	0.52(4)
(BCS: 0.576)	0.514[a]		
$\gamma T_c^2/H_c^2(0)$	0.178/0.160[c]	0.143(5)	0.14(1)
(BCS: 0.168)	0.171[a]		
$\Delta(0)/k_B T_c$	2.10(5)	2.20(5)	2.1(1)
(BCS: 1.76)	1.95[a]		

[a]Reference 17.
[b]Reference 18.
[c]Corrected value; see text.

calculated $D(t)$ functions presented in Fig. 1 of Ref. 23, $\Delta(0)/k_B T_c$ is estimated to be 2.2 and 2.1 for $LuNi_2B_2C$ and YNi_2B_2C, respectively, whilst for $LaPt_{1.5}Au_{0.5}B_2C$ only a rough estimate can be made ranging between 2.0 and 2.2.

In a previous work[12] we demonstrated for YNi_2B_2C that the electronic specific heat in the superconducting state follows a power law $C_{eS}=3\gamma T_c(T/T_c)^a$, with an exponent a close to 3, rather than the expected exponential behavior. This can qualitatively be seen from the rather linear behavior of the C_P/T versus T^2 plots of the data below T_c for all three compounds. Carter *et al.*[18] reported a similar temperature dependence of C_{eS} on $LuNi_2B_2C$ and $LaPt_{1.7}Au_{0.3}B_2C$. Therefore a determination of the gap with the BCS formula

$$C_{eS}(T)=8.5\gamma T_c \exp[-0.82\Delta(0)/k_B T] \quad (2.5<T_c/T<6)$$

cannot be performed. For a more detailed analysis of $C_{eS}(T)$ of YNi_2B_2C we refer to Ref. 12.

2. *Thermodynamic BCS ratios*

It is instructive to compare the experimental results of the dimensionless ratios $\Delta(0)/k_B\bar{T}_c$, $(\Delta C)_{Tc}/\gamma\bar{T}_c$, $h_c(0)=H_c(0)/H_c'(\bar{T}_c)\bar{T}_c$, and $\gamma\bar{T}_c^2/H_c^2(0)$ summarized in Table II and their deviations from the BCS values with λ given in Table I. As strong coupling modifies these ratios which are universal in the BCS limit but not in the Eliashberg theory, the deviations can be regarded as a measure of the coupling

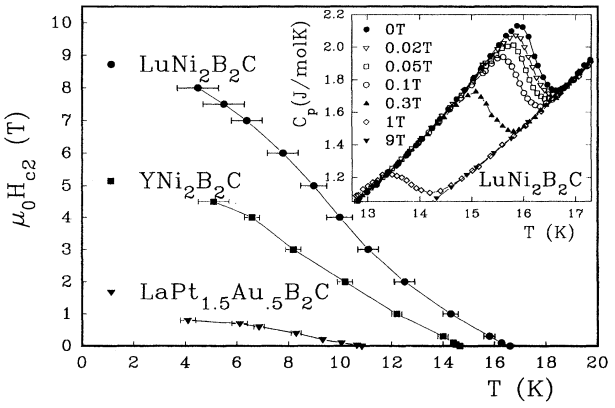

FIG. 3. Upper critical field of YNi_2B_2C, $Lu\,Ni_2B_2C$, and $LaPt_{1.5}Au_{0.5}B_2C$ as a function of temperature for various fields; inset: low-field variation of the specific-heat jump of $LuNi_2B_2C$.

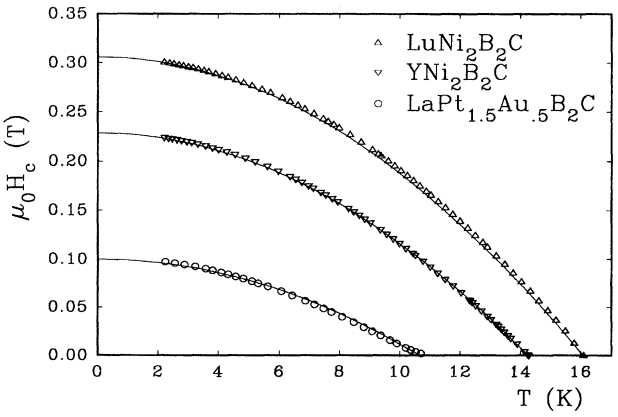

FIG. 4. Thermodynamic critical field for YNi_2B_2C, $LuNi_2B_2C$, and $LaPt_{1.5}Au_{0.5}B_2C$ determined by integrating the entropy difference between the normal state and superconducting state [see also Eq. (1)] using the data of Figs. 1(a)–1(c) and Fig. 2; the solid lines show the parabolas used to obtain the deviation functions.

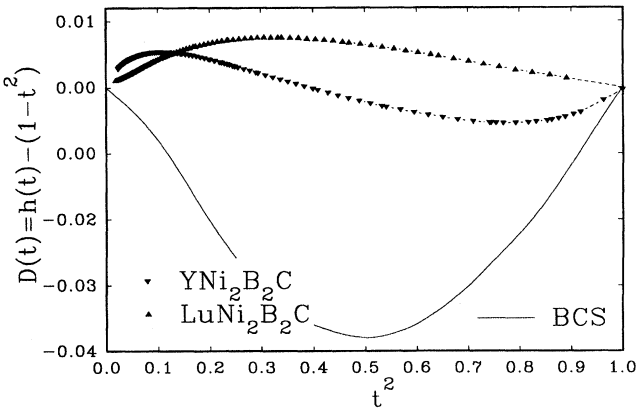

FIG. 5. Deviation function $D(t)=[H_c(t)/H_c(0)]-[1-t^2]$ for YNi_2B_2C, and $LuNi_2B_2C$ as a function of the reduced temperature $t=T/T_c$; solid line: weak-coupling (BCS) result.

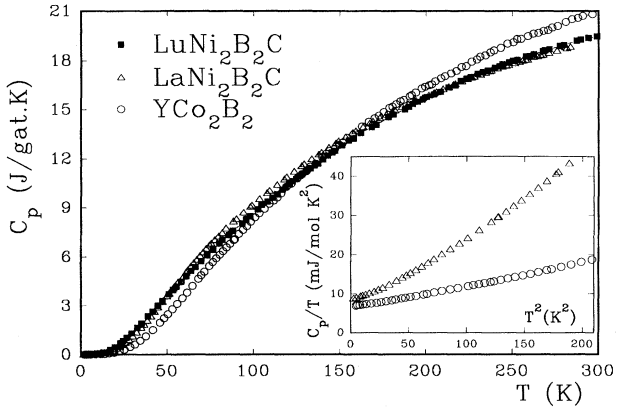

FIG. 6. Normal-state heat capacity of superconducting $LuNi_2B_2C$ and nonsuperconducting $LaNi_2B_2C$ and YCo_2B_2, inset C_P/T versus T^2 plot for both latter compounds.

strength and have been expressed as a function of the strong-coupling parameter $T_c/\omega_{\ln}$ (for a review see, e.g., Carbotte and references therein[16]). The characteristic phonon energy $\omega_{\ln}$ is the logarithmic moment of the electron-phonon spectral function $\alpha^2F(\omega)$. An increase of the coupling strength enhances the first two ratios while the latter two are reduced with respect to the BCS values given also in Table II. Note, these data are rather consistent with each other with the exception of $\gamma\bar{T}_c^2/H_c^2(0)$ for YNi_2B_2C which is beyond the BCS regime. As errors of $H_c(0)$ and $\bar{T}_c$ enter quadratically into this ratio, a correction of our $H_c(0)$ due to 5% secondary phases yields a consistent value for $\gamma\bar{T}_c^2/H_c^2(0) = 0.160$ referred to as corrected in Table II. (The same value is obtained with the single-crystal data of Movshovich[17] using a slightly reduced $\bar{T}_c=14.6$ K derived from a reanalysis of their specific-heat jump.)

According to the deviation of these three ratios from the BCS values given in Table II and the estimates for $\Delta(0)/k_BT_c$ we deduce that the coupling strength is largest for $LuNi_2B_2C$ and is slightly reduced for both YNi_2B_2C and $LaPt_{1.5}Au_{0.5}B_2C$. This tendency is not in line with the λ values derived from the ratio $\gamma/\gamma_{\text{band}}$ where λ is largest for YNi_2B_2C and rather small for $LaPt_{1.5}Au_{0.5}B_2C$ (0.1–0.3). This discrepancy is suggested to arise from the presence of electron-electron correlations and will be discussed together with λ values derived from the Allen and Dynes formula[24] in Sec. IV B.

3. *Normal-state heat capacity*

An overview of the heat capacity of superconducting $LuNi_2B_2C$ and the two nonsuperconducting reference compounds $LaNi_2B_2C$ and YCo_2B_2 in Fig. 6 displays the general low- and high-temperature features of these systems in the normal state. Note, $C_P(T)$ is given in J/gat K in order to compare the phonon contribution of YCo_2B_2 (crystallizing in the unfilled $ThCr_2Si_2$ structure) with those of the borocarbides; for the low-temperature C_P/T versus T^2 plot in the inset of Fig. 6 the unit mJ/mol K is used. From the slope of the C_P/T vs T^2 plot (which is inversely related to the low-temperature value of Θ_D^{LT}) it is obvious that the low-energy modes of the borocarbides are considerably softer than those of YCo_2B_2 whilst the crossover of the $C_P(T)$ data at about 120 K reveals a stiffening of the high-energy optical modes in the borocarbides with respect to YCo_2B_2. The former feature is also reflected by the variation of Θ_D^{LT} in these compounds (see Table I). The analysis of $C_P(T)$ in terms of a model phonon density of states $F(\omega)$ is given in the next section.

B. Numerical analysis of the heat capacity

In order to elaborate the differences in the lattice properties of the compounds investigated we analyzed their normal-state specific heat from 2 to 300 K. This temperature range is sufficient to obtain enough information about the phonon density of states $F(\omega)$ to perform a reliable calculation of the moments of the phonon spectrum, which are rather insensitive to shape details of the spectrum as shown by Junod and co-workers.[25,26]

In a previous publication[4] we gave a rough parametric description of $C_P(20-100$ K) with one Debye and two Einstein functions, but this set of parameters is too simple to account for all features of the measurements in the extended temperature range from 2 to 300 K. It is obvious that the description of $C_P(T)$ can be improved by increasing the number of Einstein functions, but this leads to ambiguous results and a loss of physical significance.

Due to the lack of reference phonon spectra from neutron or tunneling experiments we constructed a simple model spectrum $F(\omega)$ containing one Debye spectrum and three Gaussian contributions and evaluated the Einstein integrals of $F(\omega)$

$$C_{\text{ph}}(T)=\int_0^\infty F(\omega)\frac{\left(\frac{\omega}{2T}\right)^2}{\sinh^2\left(\frac{\omega}{2T}\right)}d\omega \qquad (2)$$

to obtain a satisfactory agreement with the experimental specific heat by adjusting a minimum set of free parameters. The Debye spectrum with the Debye temperature Θ_D as the free

TABLE III. Fixed parameters of the model spectrum.

Cont.	Θ_D	Θ_{E_1}	Θ_{E_2}	Θ_{E_3} (cutoff)
Width (K)		18	140	300
Weight	3	1.5	8.5	5

parameter represents the spectral weight of the three acoustic branches of the phonon spectrum (mainly determined by the specific heat at low temperatures) and three Gaussians contributions account for the 15 optical branches. The free parameters are the peak positions Θ_{E_i}. In order to obtain a high-energy limit of the phonon spectrum the Gaussian contribution with the highest energy was cut off at the peak position. Gaussians were chosen because they are smooth and easy to normalize. The "hidden" parameters of the model spectrum—the widths and weights of the Gaussian contributions to the Einstein integrals—were adjusted to obtain a satisfactory fit under the constraint of minimal variation of the hidden parameters for the compound series investigated. To avoid finite spectral density at $\omega=0$ the Einstein integrals of the Gaussian contributions were calculated from 50 K up to the cutoff energy. This leads to a negligible error in the normalization (less than 0.002), which has no influence on the moments of the spectrum. (Only in the case of $LaPt_{1.5}Au_{0.5}B_2C$ it was necessary to readjust the spectral weight of the contribution corresponding to Θ_{E_2} to 8.5.) The choice for the hidden parameters is listed in Table III. This procedure provides a satisfactory description of the $C_P(T)$ data from 2 up to 300 K shown as full lines in Fig. 8 where the logarithmic representation is used to emphasize the distinct features of the low- and medium-temperature normal-state heat capacity of this compound series. (For the superconducting compounds $LuNi_2B_2C$, YNi_2B_2C, and $LaPt_{1.5}Au_{0.5}B_2C$, the normal-state data of the 9 T measurements are shown; the data of the nonsuperconducting $LaNi_2B_2C$ are not included for clarity, since they are situated just in between $LuNi_2B_2C$ and YNi_2B_2C.)

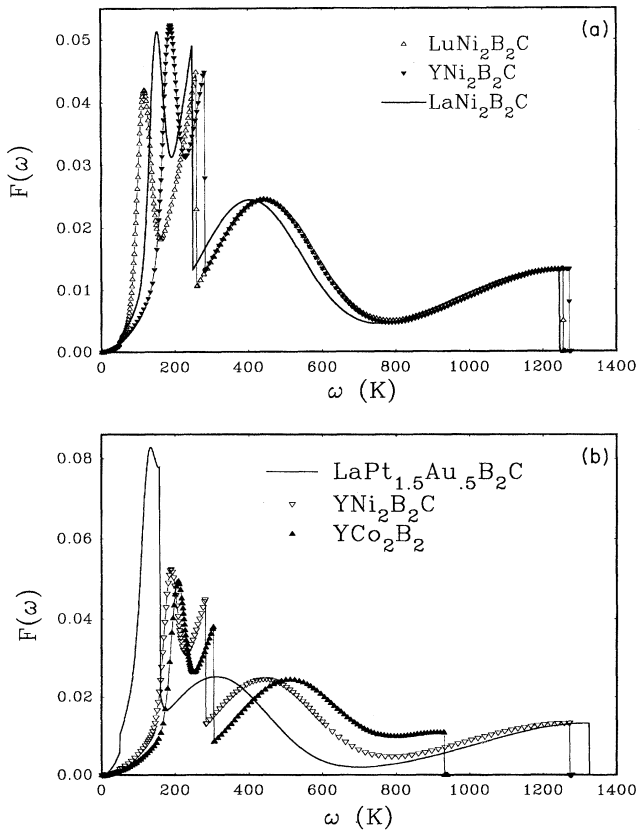

FIG. 7. Model phonon spectra $F(\omega)$ for YNi_2B_2C, $LuNi_2B_2C$, and $LaNi_2B_2C$ (a) and the same for $LaPt_{1.5}Au_{0.5}B_2C$, YNi_2B_2C, and YCo_2B_2 (b).

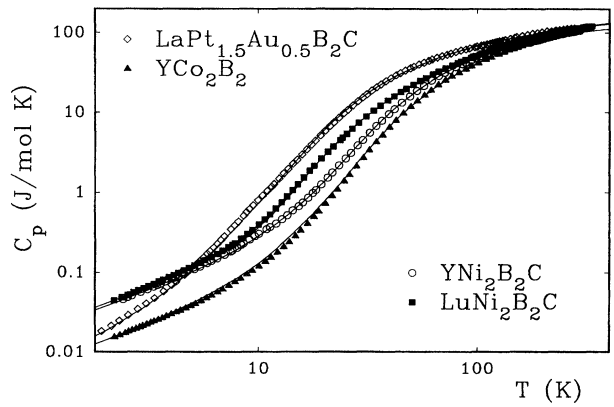

FIG. 8. Normal-state heat capacity of superconducting YNi_2B_2C, $LuNi_2B_2C$, $LaPt_{1.5}Au_{0.5}B_2C$, and nonsuperconducting YCo_2B_2; solid lines represent the fit of the model phonon spectra $F(\omega)$ [see Figs. 7(a) and 7(b)] to $C_P(T)$ according to Eq. (2).

The corresponding model spectra $F(\omega)$ are displayed in Figs. 7(a) and 7(b) and the numerical results of the characteristic temperatures are summarized in Table IV. A remarkable feature of the model spectra is the sharp low-frequency contribution (Θ_{E_1}) with a weight of 1.5. If this weight is changed it is hardly possible to describe the distinct low-temperature features of the heat capacities in Fig. 8 and the associated curvatures of the C_P/T vs T^2 plots in Figs. 1(a)–1(c) and Fig. 6 inset at about 80, 120, and 80 K^2 for $LuNi_2B_2C$, YNi_2B_2C, and $LaNi_2B_2C$, respectively. From the comparison of the characteristic temperatures and the model spectra one can hardly deduce a decisive hint for the disappearance of superconductivity in $LaNi_2B_2C$: Its low-frequency contribution (Θ_{E_1}) is situated in between those of the superconducting compounds and the high-frequency

TABLE IV. Numerical results of the model spectrum fit to the measured heat capacities.

	Θ_D (K)	Θ_{E_1} (K)	Θ_{E_2} (K)	Θ_{E_3} (K)
YNi_2B_2C	282	187	439	1272
$LuNi_2B_2C$	260	117	441	1257
$LaNi_2B_2C$	250	151	404	1246
$LaPt_{1.5}Au_{0.5}B_2C$	159	127	310	1325
YCo_2B_2	304	207	507	931

modes of these three compounds have nearly the same energies. In the case of $LaPt_{1.5}Au_{0.5}B_2C$ the Debye contribution (Θ_D) is situated at about 160 K, close to the low-energy Einstein contribution (Θ_{E1}) and causes a rather prominent maximum in the phonon density of states displayed in Fig. 7(b). In comparison to the Ni compounds the latter spectrum describes a much softer lattice.

A significant difference of the lattice properties between the filled and unfilled version of the $ThCr_2Si_2$ structure emerges from the comparison of the model phonon spectra of YNi_2B_2C and YCo_2B_2 also displayed in Fig. 7(b). With regard to the missing light carbon atom in YCo_2B_2, the corresponding spectral weight of the high-energy contribution (Θ_{E_3}) was reduced from five to two and simultaneously the width of this part of the model spectrum was reduced to 150 K, because the flat high-energy contribution of the borocarbides cannot account for the high-temperature specific heat of YCo_2B_2. This modification yields the model spectrum of YCo_2B_2 where the high-energy cutoff is significantly decreased to 930 K but the low-frequency modes are shifted to higher energies. The latter is also evident from a comparison of the low-temperature $\Theta_D^{\rm LT}$ values of YNi_2B_2C [$\Theta_D^{\rm LT}$= 490(5) K] and YCo_2B_2 [$\Theta_D^{\rm LT}$= 570(10) K] indicating an overall lattice stiffening in the low-temperature regime, whilst the high-frequency modes soften which is also evident from the crossover of the $C_P(T)$ data in Fig. 6.

The phonon spectrum of YNi_2B_2C can be compared with the results of Raman spectroscopy reported by Hadjiev *et al.*[27] They detected four Raman-active modes with the energies corresponding to 285 K (B_{1g}), 406 K (E_{1g}), 676 K (E_g), and 1197 K (A_{1g}). The high-energy mode coincides quite well with the cutoff temperature of the fit and supports the applicability of the model spectrum proposed.

Comparison of a characteristic phonon frequency $\tilde{\omega}$ with the model spectrum

Kresin and Parkhomenko[28] demonstrated that several thermodynamic properties of strong-coupling superconductors can be described in terms of the ratio $T_c/\tilde{\omega}$. For a very simple phonon spectrum, consisting of sharp well separated maxima, the characteristic phonon frequency $\tilde{\omega}$ corresponds to the energy of the first prominent maximum of the electron-phonon spectral function $\alpha^2F(\omega)$. If corrections proportional to $(T_c/\omega)^2$ due to contributions of higher energies have to be taken into account, the value of $\tilde{\omega}$ might be slightly higher. Applying the formula

$$\frac{(\Delta C)_{T_c}}{\gamma T_c}=1.43\left[1+1.8\left(\ln\frac{\tilde{\omega}}{T_c}+0.5\right)\left(\frac{\pi T_c}{\tilde{\omega}}\right)^2\right] \quad (3)$$

to the experimental values of the normalized specific-heat jump $(\Delta C)_{T_c}/\gamma T_c$, we obtain $\tilde{\omega}\approx$ 200 and 150 K for YNi_2B_2C and $LuNi_2B_2C$, respectively. These values are in agreement with those resulting from the model spectra (see Θ_{E_1} in Table IV).

A similar formula for the strong-coupling correction to the normalized gap ratio by Geilikman and Kresin:[29]

TABLE V. Estimates for the superconducting gap.

	α model	Eq. (4)	Eq. (13)
YNi_2B_2C	2.10(5)	1.90	1.95(8)
$LuNi_2B_2C$	2.20(5)	2.11	2.09(8)
$LaPt_{1.5}Au_{0.5}B_2C$	2.1(1)	1.92	2.05(10)

$$\frac{\Delta(0)}{k_BT_c}=1.76\left[1+5.3\left(\frac{T_c}{\tilde{\omega}}\right)^2\ln\left(\frac{\tilde{\omega}}{T_c}\right)\right] \quad (4)$$

yields $\Delta(0)/k_BT_c\equiv 2.11$ and 1.90 for $LuNi_2B_2C$ and YNi_2B_2C, respectively, taking $\tilde{\omega}(\approx\Theta_{E_1})$ from our model spectra. Table V gives an overview for the estimates of $\Delta(0)/k_BT_c$ according to the α model (Sec. III A 1), Eqs. (4) and (13). Although Eq. (13) is given in Sec. IV A and contains $T_c/\omega_{\ln}$ which will be evaluated in the next section, we present these results in Table V for the convenience of a comparison since both expressions are of similar shape. Ekino *et al.*[30] performed tunneling measurements on YNi_2B_2C and reported $\Delta(4.2{\rm K})/k_BT_c\approx 1.8$ which is in reasonable agreement with the estimates collected in Table V.

IV. DISCUSSION

A. Analysis of the thermodynamic ratios in terms of the strong-coupling corrections to the BCS values

The ratio between the critical temperature and a quantity representing a characteristic phonon frequency such as, e.g., Θ_D (Ref. 32) or $\tilde{\omega}$ (Ref. 28) [see Eqs. (3), (4)] has been used for a discussion of the coupling strength by various authors. Rainer and Bergmann[14] applied the Eliashberg theory for strong-coupling superconductors to several realistic superconductors and demonstrated that the magnitude of the deviations of the critical fields from BCS predictions can be estimated from the ratio $T_c/\bar{\omega}_1$ with $\bar{\omega}_1$ the first generalized moment of the electron-phonon spectral function $\alpha^2(\omega)F(\omega)$. The moments of $\alpha^2(\omega)F(\omega)$ are defined as[24]

$$\langle\omega^n\rangle=\frac{2}{\lambda}\int_0^\infty d\omega\alpha^2(\omega)F(\omega)\omega^{n-1}. \quad (5)$$

The electron-phonon interaction parameter λ is a dimensionless measure of the coupling strength

$$\lambda=2\int_0^\infty d\omega\frac{\alpha^2(\omega)F(\omega)}{\omega}. \quad (6)$$

The logarithmic average frequency $\omega_{\ln}$, equal to the $n\rightarrow 0$ limit of the sequence of average frequencies

$$\bar{\omega}_n\equiv\langle\omega^n\rangle^{1/n} \quad (7)$$

can be written in the form

$$\omega_{\ln}\equiv\lim_{n\rightarrow 0}\bar{\omega}_n=\exp\left(\frac{2}{\lambda}\int_0^\infty\frac{d\omega}{\omega}\alpha^2F(\omega)\ln(\omega)\right). \quad (8)$$

In the framework of the Eliashberg theory, using a square-well model for the gap, Marsiglio and Carbotte[15] (see also

TABLE VI. Generalized moments of the electron-phonon spectral function.

	YNi_2B_2C			$LuNi_2B_2C$			$LaNi_2B_2C$			$LaPt_{1.5}Au_{0.5}B_2C$		
$\alpha^2(\omega)\propto\omega^s$	$\omega_{\ln}$(K)	$\bar{\omega}_1$(K)	$\bar{\omega}_2$(K)	$\omega_{\ln}$(K)	$\bar{\omega}_1$(K)	$\bar{\omega}_2$(K)	$\omega_{\ln}$(K)	$\bar{\omega}_1$(K)	$\bar{\omega}_2$(K)	$\omega_{\ln}$(K)	$\bar{\omega}_1$(K)	$\bar{\omega}_2$(K)
$s=-1/2$	220	279	351	173	232	311	187	241	312	123	165	235
$s=0$	279	351	438	232	312	408	241	311	401	163	229	335
$s=-1$	164	218	277	131	175	234	138	186	240	88	122	167

Ref. 16 for a review and references therein) derived approximate formulas for the strong-coupling corrections to the dimensionless BCS ratios:

$$\frac{(\Delta C)_{T_c}}{\gamma T_c}=1.43\left[1+53\left(\frac{T_c}{\omega_{\ln}}\right)^2\ln\left(\frac{\omega_{\ln}}{3T_c}\right)\right], \tag{9}$$

$$\frac{\gamma T_c^2}{H_c^2(0)}=0.168\left[1-12.2\left(\frac{T_c}{\omega_{\ln}}\right)^2\ln\left(\frac{\omega_{\ln}}{3T_c}\right)\right], \tag{10}$$

$$h_c(0)=0.576\left[1-13.4\left(\frac{T_c}{\omega_{\ln}}\right)^2\ln\left(\frac{\omega_{\ln}}{3.5T_c}\right)\right], \tag{11}$$

$$\frac{\Delta(0)}{k_BT_c}=1.76\left[1+12.5\left(\frac{T_c}{\omega_{\ln}}\right)^2\ln\left(\frac{\omega_{\ln}}{2T_c}\right)\right]. \tag{12}$$

The strong-coupling variable is the ratio $T_c/\omega_{\ln}$ with the average phonon frequency $\omega_{\ln}$ given by Eq. (8). It was shown[16] that these equations provide a satisfactory description of the strong-coupling corrections to the BCS ratios for a large number of electron-phonon-mediated superconductors with an accuracy of about 10%. Entering the experimentally determined thermodynamic ratios in Eqs. (9)–(12), we evaluate the ratios $T_c/\omega_{\ln}$ and obtain a rough estimate for $\omega_{\ln}$ which is about 240 K for YNi_2B_2C, 160 K for $LuNi_2B_2C$, and 130 K in the case of $LaPt_{1.5}Au_{0.5}B_2C$. In order to estimate the generalized moments $\bar{\omega}_1$ and $\bar{\omega}_2$ which are, e.g., needed to determine the ratio $\bar{\omega}_2/\omega_{\ln}$ for the shape factor of the Allen and Dynes formula (see below), one has to assume a reasonable frequency dependence of $\alpha^2(\omega)$ in Eqs. (5)–(8).

The simplest assumption is a frequency independent $\alpha^2(\omega)$. Since this approximation yields $\omega_{\ln}$ values which are larger than the above given estimates (unambiguously too large for $LuNi_2B_2C$), the use of decreasing functions for $\alpha^2(\omega)$ seems to be reasonable. Thus we follow the approach of Junod *et al.*[26] They suggested the approximation $\alpha^2(\omega)\propto\omega^{-1/2}$ and used the assumptions $\alpha^2(\omega)\propto 1$ and $\alpha^2(\omega)\propto\omega^{-1}$ as limiting cases for the calculation of $\omega_{\ln}$, $\bar{\omega}_1$, and $\bar{\omega}_2$. The corresponding results for the average frequencies $\omega_{\ln}$, $\bar{\omega}_1$, and $\bar{\omega}_2$ with the proposed assumptions on the frequency dependence of α^2 are summarized in Table VI.

The thermodynamic ratios given in Table II are displayed in Fig. 9 to classify the coupling strength of the compounds investigated. The solid lines in Figs. 9(a)–9(d) represent the general trend according to Eqs. (10)–(13) typical for many superconductors which allow an apparent graphical comparison with our results for the borocarbides. The open symbols displayed in Figs. 9(a)–9(d) correspond to $\omega_{\ln}$ values determined under the assumption of $\alpha^2(\omega)\propto\omega^{-1/2}$ and the associated horizontal error bars correspond to $\omega_{\ln}$ values determined with $\alpha^2(\omega)\propto\omega^{-1}$ and $\alpha^2(\omega)\propto 1$, respectively. Figure 9 further illustrates that the coupling strength of these three superconductors is of the same magnitude and decreases slightly in the sequence: $LuNi_2B_2C$, $LaPt_{1.5}Au_{0.5}B_2C$, and YNi_2B_2C.

The $\bar{\omega}_1$ values of Table VI can be compared with the theoretical predictions of Rainer and Bergmann[14] for the magnitude of the strong-coupling correction of the thermodynamic critical field H_c from BCS at given ratios of $T_c/\bar{\omega}_1$. The numerical results for the enhancement parameters $\eta_{H_c}(T_c)$ and $\eta_{H_c}(0)$ of the thermodynamic critical field

$$H_c(T)=\eta_{H_c}(T)H_c^{\mathrm{BCS}}(T) \tag{13}$$

as well as $\eta_{H_{c2}}(T_c)$ and $\eta_{H_{c2}}(0)$, the enhancement parameters of the upper critical field, can be deduced from Fig. 1 of Ref. 14. Calculations for the upper critical field have been performed in the dirty-limit approximation, which cannot be applied to the RNi_2B_2C compounds because they are clean-limit superconductors.[31]

The experimental values of the enhancement parameters $\eta_{H_c}(0)$ and $\eta_{H_c}(T_c)$ were determined from the relations $\gamma T_c^2/H_c^2(0)=0.168\,\eta_{H_c}^{-2}(0)$ and $(\Delta C)_{T_c}/\gamma T_c=1.43\,\eta_{H_c}^2(T_c)$. Table VII contains our experimental enhancement factors of the thermodynamic critical field and those taken from Rainer and Bergmann[14] for the $T_c/\bar{\omega}_1$ values corresponding to Table VI. The comparison of the data in Table VII reveals that the approximation $\alpha^2\propto\omega^{-1/2}$ appears to be a reasonable approach.

B. Determination of the electron-phonon interaction parameter

For the evaluation of λ we use the Allen and Dynes formula[24] with a Coulomb pseudopotential $\mu^*=0.13$ (see, e.g., Ref. 32)

$$T_c=\frac{f_1f_2\omega_{\ln}}{1.20}\exp\left(-\frac{1.04(1+\lambda)}{\lambda-\mu^*-0.62\lambda\mu^*}\right), \tag{14}$$

where f_1 and f_2 are corrective factors given by

$$f_1=\left[1+\left(\frac{\lambda}{2.46(1+3.8\mu^*)}\right)^{\frac{3}{2}}\right]^{\frac{1}{3}}, \tag{15}$$

$$f_2=1+\frac{\left(\frac{\bar{\omega}_2}{\omega_{\ln}}-1\right)\lambda^2}{\lambda^2+1.82(1+6.3\mu^*)\frac{\bar{\omega}_2}{\omega_{\ln}}}. \tag{16}$$

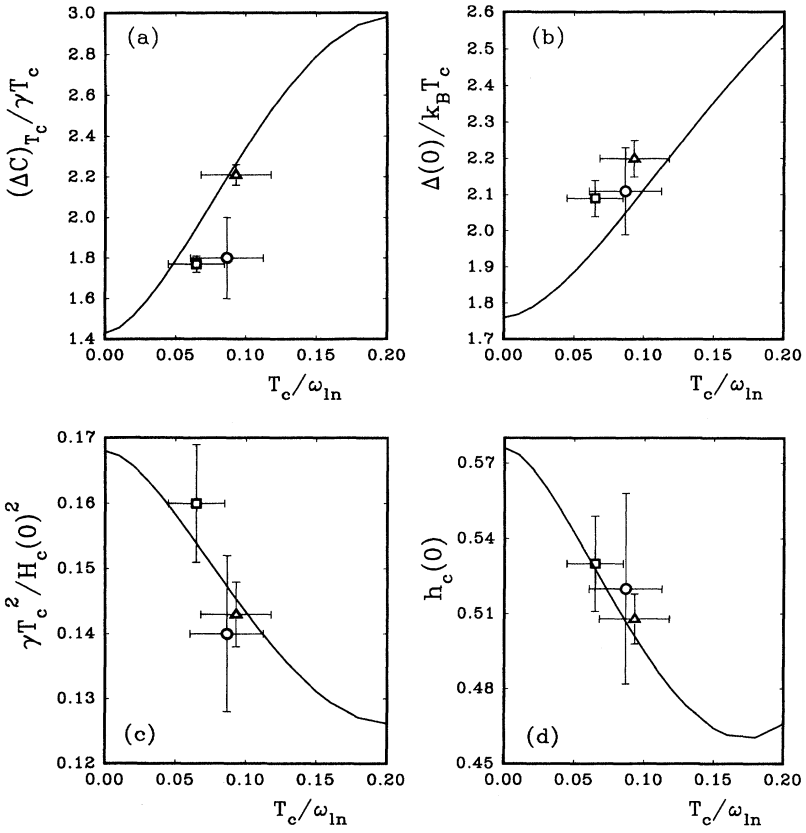

FIG. 9. (a)–(d) Strong-coupling correction to the dimensionless BCS ratios $(\Delta C)_{T_c}/\gamma T_c$, $\Delta(0)/k_B T_c$, $\gamma T_c^2/H_c^2(0)$, and $h_c(0)$ as a function of the strong-coupling variable T_c/ω_{ln} for YNi_2B_2C (□), $LuNi_2B_2C$ (△), and $LaPt_{1.5}Au_{0.5}B_2C$ (○).

For the three superconducting compounds we obtain λ values of about 1, while for $LaNi_2B_2C$ only an upper limit ($\lambda<0.5$) can be estimated since it is nonsuperconducting down to 1.5 K. It should be noted that due to the large ratio $\bar{\omega}_2/\omega_{ln}\sim 1.8$ the McMillan formula[32] yields λ values by about 20% smaller than those from the Allen and Dynes expression. These λ values labeled as λ_{AD} and the average of the function $\alpha^2(\omega)$, $\bar{\alpha}^2\equiv(1/2)\lambda\bar{\omega}_1$, are listed in Table VIII together with those given in Table I that were determined from the ratio $\gamma_{exp}/\gamma_{band}=(1+\lambda_{tot})$. As the latter contain the total mass enhancement (electron correlations and electron-phonon interaction), λ_{tot} should be larger than λ_{AD}. Hence, the difference between both sets of λ values in Table VIII indicates that band-structure calculations overestimate $N(E_f)$. This is in agreement with conclusions from spectroscopic measurements[9–11] where the calculated DOS peak at E_f is found to be reduced by electron correlations. On the other hand we concluded[4] in agreement with Carter *et al.*[18] from the comparison of the Pauli susceptibility with γ values and band-structure data that the static susceptibility is not significantly enhanced.

Although the general trend of the variation of γ_{band} within this compound series qualitatively follows that of γ_{exp}, it is remarkable that the largest discrepancy between the two sets of λ is found for $LaPt_{1.5}Au_{0.5}B_2C$ ($\lambda=0.1$ and 1.1) where we observe a significant field dependence of the low-temperature normal-state heat capacity which may arise from spin fluctuations. For $LaPt_{1.5}Au_{0.5}B_2C$, $\lambda_{AD}=1.1$ appears to be of reasonable magnitude being in agreement with its coupling strength T_c/ω_{ln} (Fig. 9), while $\lambda_{tot}=0.1$ can be regarded as too small because not even $\lambda\sim 0.3$ can account for superconductivity above the mK regime using the phonon frequencies from Table VI.

The T_c reduction of $LaPt_{1.5}Au_{0.5}B_2C$ with respect to the superconducting Ni compounds and the disappearance of superconductivity in $LaNi_2B_2C$ is reflected in the variation of

TABLE VII. Comparison the enhancement factors of the thermodynamic critical field obtained from theory and specific heat.

	YNi_2B_2C		$LuNi_2B_2C$	
	$\eta_{H_c}(0)$	$\eta_{H_c}(T_c)$	$\eta_{H_c}(0)$	$\eta_{H_c}(T_c)$
Expt.	1.02(2)	1.12(1)	1.08(2)	1.23(1)
$\alpha^2\propto\omega^{-1/2}$	1.04	1.13	1.06	1.19
$\alpha^2\propto 1$	1.03	1.09	1.04	1.13
$\alpha^2\propto\omega^{-1}$	1.06	1.19	1.09	1.27

TABLE VIII. Comparison of the electron-phonon mass enhancement factors $\lambda_{tot}(=\gamma_{exp}/\gamma_{band}-1)$ with λ_{AD} and the average value $\bar{\alpha}^2(=1/2\lambda_{AD}\bar{\omega}_1)$.

	λ_{tot}	λ_{AD}	$\bar{\alpha}^2$
YNi_2B_2C	0.9	0.95(5)	133(7)
$LuNi_2B_2C$	0.75	1.15(5)	133(7)
$LaNi_2B_2C$	0.4	<0.5	<60
$LaPt_{1.5}Au_{0.5}B_2C$	0.1	1.1(1)	100(10)

$\bar{\alpha}^2 \equiv (1/2)\lambda\bar{\omega}_1$. Although it is difficult to disentangle the phononic and electronic contribution one can use the relation $\lambda = N(E_f)\langle I^2\rangle/(M\bar{\omega}_2^2)$ for a qualitative discussion (with $\langle I^2\rangle$ the average of the electron-phonon matrix elements and M the mean atomic mass). The denominator, a phonon quantity, varies for these four compounds only by about 10% and is similar to the relative variation of λ_{AD} for the three superconducting compounds which implies that the nominator, the electronic Hopfield parameter η, remains approximately constant for $LuNi_2B_2C$, YNi_2B_2C, and $LaPt_{1.5}Au_{0.5}B_2C$, although γ of the latter is by 65% smaller than γ of the two other superconductors. Hence, the softening of the low-frequency modes, represented by ω_{ln}, has a detrimental effect upon T_c of $LaPt_{1.5}Au_{0.5}B_2C$. On the other hand, the disappearance of superconductivity in $LaNi_2B_2C$ may be associated with the reduced DOS at E_f, since the overall feature of our model phonon spectra is rather similar for $LaNi_2B_2C$, YNi_2B_2C, and $LuNi_2B_2C$.

In this context it is of interest that Mattheiss *et al.*[33] attributed the superconducting properties to an electron-phonon mechanism in which high-frequency boron A_{1g} phonons couple strongly to an energy band of the Ni-B-C manifold whose position is sensitive to the geometry of the NiB_4 tetrahedron and modulate the Ni-B-Ni bond angle. It is proposed that superconductivity occurs only when a special s-p band is optimally aligned to E_f which happens to occur for nearly ideal NiB_4 angles in YNi_2B_2C and $LuNi_2B_2C$ concomitant with a high DOS at E_f. As a result of the deviation from the idealized structure due to the larger La ionic radius with respect to Lu or Y the relevant s-p band is shifted to higher energies yielding a reduction of $N(E_f)$ by -47% for $LaNi_2B_2C$ with respect to $LuNi_2B_2C$. This is in agreement with the experiment where we observe a reduction of -57% (see Table I). However, the low characteristic frequencies $\bar{\omega}_1$ and ω_{ln} (Table VI), derived from our model phonon spectra which provides a satisfactory description of the strong-coupling corrections, seem to contradict the suggestion of Mattheiss *et al.*[33] that the mechanism for superconductivity is based on high-frequency boron A_{1g} optical phonons with energies equivalent to 1200 K.

C. The upper critical field

In order to quantitatively examine the upward curvature of $H_{c2}(T)$ we plot in Fig. 10 the normalized upper critical field $h_{c2}(T) = H_{c2}(T)/(T_c dH_{c2}/dT)_{T_c}$ as a function of the reduced temperature $t = T/T_c$ together with the weak-coupling result labeled as "BCS." From the temperature dependence of the thermodynamic and upper critical field (in Figs. 3 and 4) one obtains the normalized ratio $k(T) = \kappa_1(T)/\kappa_1(T_c)$ of the Ginzburg-Landau parameter $\kappa_1(T) = H_{c2}(T)/\sqrt{2}H_c(T)$ displayed in the inset of Fig. 10. The data of $LaPt_{1.5}Au_{0.5}B_2C$ are close to the BCS result but exhibit considerable scatter and are therefore not shown. The extrapolated values for $k(0) = \kappa_1(0)/\kappa_1(T_c)$ are about 1.5(1), 2.0(1), and 1.3(3) for YNi_2B_2C, $LuNi_2B_2C$, and $LaPt_{1.5}Au_{0.5}B_2C$, respectively. The former two are significantly enhanced with respect to the weak-coupling ("BCS") result in the clean limit (1.26). Carbotte[16] showed that $h_{c2}(0)$ and $k(0)$ follow approximate relations that contain the strong-coupling correction $(T_c/\omega_{ln})^2 \ln(\omega_{ln}/bT_c)$ in a similar way to Eqs. (10)–(13) for the dimensionless BCS ratios. A comparison of $k(0)$ with the data compiled in Ref. 16 of a large number of electron-phonon-mediated superconductors, which are in the range $0 < T_c/\omega_{ln} < 0.2$ for $1.2 < k(0) < 1.8$ shows that $k(0) = 1.5$ yields T_c/ω_{ln} of about 0.15 for YNi_2B_2C while a remarkably high $T_c/\omega_{ln} > 0.2$ would be required to account for $k(0) \simeq 2$ of $LuNi_2B_2C$. Both values are significantly higher than the rather consistent T_c/ω_{ln} values derived from the four dimensionless ratios [Eqs. (10)–(13)] ranging between 0.06 and 0.1. Not even very strong coupling can account for the pronounced upward curvature and enhancement of $h_{c2}(0)$ for $LuNi_2B_2C$ which is reminiscent of a calculation using a δ-function-based phonon spectrum with $T_c/\omega_E \simeq 1$ (Ref. 16) where ω_E is the Einstein frequency of the δ function. However, a dominant Einstein frequency at about 15 K is not compatible with the specific-heat data from which we obtain $\Theta_{E1} = 117$ K as the low-frequency Einstein mode for $LuNi_2B_2C$.

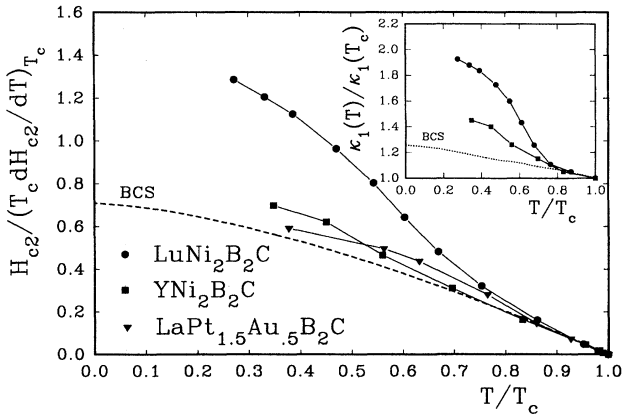

FIG. 10. Normalized upper critical field $h_{c2}(T) = H_{c2}(T)/(T_c dH_{c2}/dT)_{Tc}$ as a function of the reduced temperature T/T_c for YNi_2B_2C, $LuNi_2B_2C$, and $LaPt_{1.5}Au_{0.5}B_2C$; inset: normalized Ginzburg-Landau parameter for YNi_2B_2C, $LuNi_2B_2C$; dashed lines: weak-coupling BCS result for a comparison.

Although various properties in the superconducting state of these borocarbides can be explained rather consistently with the model phonon spectra, the significant upturn of $h_{c2}(0)$ and the enhancement of the normalized Ginzburg-Landau parameter remain to be resolved.

V. CONCLUSION

We determined the thermodynamic BCS ratios of YNi_2B_2C, $LuNi_2B_2C$, and $LaPt_{1.5}Au_{0.5}B_2C$ from specific-heat measurements and deduced according to their deviation from the weak-coupling BCS values the strong-coupling correction in terms of T_c/ω_{ln}.

From the normal-state specific heat between 2 and 300 K of these superconductors and the nonsuperconducting reference compounds $LaNi_2B_2C$ and YCo_2B_2 we constructed model phonon spectra yielding the moments of the phonon density of states $F(\omega)$. A remarkable reduction of the high-frequency modes is obtained for YCo_2B_2 with respect to the borocarbides investigated due to the missing carbon atoms in

the former. The model phonon spectra of the superconducting compounds YNi_2B_2C, $LuNi_2B_2C$, and $LaPt_{1.5}Au_{0.5}B_2C$ are (with the exception of a softening of the low-frequency modes of the latter) essentially the same as for nonsuperconducting $LaNi_2B_2C$. The former three compounds can be classified as moderately strong coupled superconductors since the electron-phonon enhancement parameter λ derived from the Allen and Dynes formula ranges between 0.95 and 1.15.

The difference between these λ values and those deduced from $\gamma_{exp}/\gamma_{band}$ shows that band-structure calculations overestimate $N(E_f)$ in particular for $LaPt_{1.5}Au_{0.5}B_2C$ and that electron-electron correlations may be important. As the λ values from the Allen and Dynes formula are of the same magnitude for the three superconducting compounds, the lower T_c of $LaPt_{1.5}Au_{0.5}B_2C$ is suggested to be associated with the softening of the low-frequency modes, while the disappearance of superconductivity in $LaNi_2B_2C$ may be attributed to the smaller γ value reduced by about 50% with respect to those of YNi_2B_2C and $LuNi_2B_2C$. This reduction of $N(E_f)$ is in agreement with band-structure calculations and was attributed to the deviation from the ideal NiB_4 tetrahedral angle by Mattheiss *et al.*[33] For YNi_2B_2C and especially $LuNi_2B_2C$ our data reveal an anomalous upward curvature of $H_{c2}(T)$ and $\kappa_1(T)/\kappa_1(T_c)$ which cannot be described in terms of the strong-coupling corrections T_c/ω_{ln} and remains to be resolved.

ACKNOWLEDGMENTS

We are indebted to N.M. Hong and M. Vybornov for their support in sample preparation and x-ray characterization. This work was supported by the Austrian Science Foundation under Grants No. 11090, S5604, and by the Kärntner Elektrizitätsgesellschaft (KELAG).

[1] R. J. Cava, H. Takagi, H. W. Zandbergen, J. J. Krajewski, W. F. Peck, Jr., T. Sigrist, B. Batlogg, R. B. van Dover, R. J. Felder, K. Mizuhashi, J. O. Lee, H. Eisaki, and S. Uchida, Nature (London) **367**, 254 (1994).

[2] R. Nagarajan, C. Mazumdar, Z. Hossain, S. K. Dhar, K. V. Gopalakrishnan, L. C. Gupta, C. Godart, B. D. Padalia, and R. Vijayaraghavan, Phys. Rev. Lett. **72**, 274 (1994).

[3] T. Siegrist, H. W. Zandbergen, R. J. Cava, J. J. Krajewski, and W. F. Peck, Jr., Nature (London) **367**, 146 (1994).

[4] G. Hilscher, H. Michor, N. M. Hong, W. Perthold, M. Vybornov, and P. Rogl, Physica B **206 & 207**, 542 (1995).

[5] L. F. Mattheiss, Phys. Rev. B **49**, 13 279 (1994).

[6] W. E. Pickett and D. J. Singh, Phys. Rev. Lett. **72**, 3702 (1994).

[7] J. I. Lee, T. S. Zhao, I. G. Kim, B. I. Min, and S. J. Youn, Phys. Rev. B **50**, 4030 (1994).

[8] D. J. Singh, Phys. Rev. B **50**, 6486 (1994).

[9] A. Fujimori, K. Kobayashi, T. Mizokawa, K. Mamiya, and A. Sekiyama, Phys. Rev. B **50**, 9660 (1994).

[10] M. S. Golden, M. Kupfer, M. Kielwein, M. Buchgeister, J. Fink, D. Teehan, W. E. Pickett, and D. J. Singh, Europhys. Lett. **28**, 369 (1994).

[11] E. Pellegrin, C. T. Chen, G. Meigs, R. J. Cava, J. J. Krajewski, and W. F. Peck, Jr., Phys. Rev. B **51**, 16 159 (1995).

[12] N. M. Hong, H. Michor, M. Vybornov, T. Holubar, P. Hundegger, W. Perthold, G. Hilscher, and P. Rogl, Physica C **227**, 85 (1994).

[13] R. J. Cava, B. Batlogg, J. J. Krajewski, F. W. Peck, Jr., T. Sigrist, R. M. Fleming, S. Carter, H. Takagi, R. J. Felder, R. V. van Dover, and L. W. Rupp, Jr., Physica C **226**, 170 (1994).

[14] D. Rainer and G. Bergmann, J. Low Temp. Phys. **14**, 501 (1974).

[15] F. Marsiglio and J. P. Carbotte, Phys. Rev. B **33**, 6141 (1986).

[16] J. P. Carbotte, Rev. Mod. Phys. **62**, 1027 (1990).

[17] R. Movshovich, M. F. Hundley, J. D. Thompson, P. C. Canfield, B. K. Cho, and A. V. Chubukov, Physica C **227**, 381 (1994).

[18] S. A. Carter, B. Batlogg, R. J. Cava, J. J. Krajewski, and W. F. Peck, Jr., Phys. Rev. B **50**, 4216 (1994).

[19] J. S. Kim, W. W. Kim, and G. R. Stewart, Phys. Rev. B **50**, 3485 (1994).

[20] C. Godart, L. C. Gupta, R. Nagarajan, S. K. Dhar, H. Noel, M. Potel, C. Mazumdar, Z. Hossain, C. Levy-Clement, G. Schiffmacher, B. D. Padalia, and R. Vijayaraghavan, Phys. Rev. B **51**, 489 (1995).

[21] R. Cywinski, Z. P. Han, R. Bewley, R. Cubitt, M. T. Wylie, E. M. Forgan, S. L. Lee, M. Warden, and S. H. Kilcoyne, Physica C **233**, 273 (1994).

[22] Ming Xu, P. C. Canfield, J. E. Ostenson, D. K. Finnemore, B. K. Cho, Z. R. Wang, and D. C. Johnson, Physica C **227**, 321 (1994).

[23] H. Padamsee, J. E. Neighbor, and C. A. Shiffman, J. Low Temp. Phys. **12**, 387 (1973).

[24] P. B. Allen and R.C. Dynes, Phys. Rev. B **12**, 905 (1975).

[25] A. Junod, T. Jarlborg, and J. Muller, Phys. Rev. B **27**, 1568 (1983).

[26] A. Junod, D. Bichsel, and J. Muller, Helv. Phys. Acta **52**, 580 (1979).

[27] V. G. Hadjiev, L. N. Bozukov, and M. G. Baychev, Phys. Rev. B **50**, 16 726 (1994).

[28] V. Z. Kresin and V. P. Parkhomenko, Fiz. Tverd. Tela (Leningrad) **16**, 3363 (1974) [Sov. Phys. Solid State **16**, 2180 (1975)].

[29] B. T. Geilikman and V. Z. Kresin, Fiz. Tverd. Tela (Leningrad) **7**, 3294 (1965) [Sov. Phys. Solid State **7**, 2659 (1966)].

[30] T. Ekino, H. Fujii, M. Kosugi, Y. Zenitani, and J. Akimitsu, Physica C **235-240**, 2529 (1994).

[31] H. Takagi, R. J. Cava, H. Eisaki, J. O. Lee, K. Mizuhashi, B. Batlogg, S. Uchida, J. J. Krajewski, and W. F. Peck, Jr., Physica C **228**, 389 (1994).

[32] W. L. McMillan, Phys. Rev. **167**, 331 (1968).

[33] L. F. Mattheiss, T. Siegrist, and R. J. Cava, Solid State Commun. **91**, 587 (1994).